Reliability-guaranteed admission control for mobile computation offloading under Nakagami fading channel

Article (Accepted Version)

Reliability-Guaranteed Admission Control for Mobile Computation Offloading under Nakagami Fading Channel

Guixian Qu, Jianshan Zhou, Zhengguo Sheng, *Senior Member, IEEE*, Haiyang Yu, and Yilong Ren

***Abstract*—The coupled stochastic channel interferences can lead to intermittent connectivity and invalid fragment transmissions, which pose a significant challenge to guarantee the reliability of computation offloading. A wide variety of conventional approaches to making offloading decisions are based on the fundamental condition that channels are sufficiently reliable for completing each transmission session. However, the reliability that a user can successfully offload a computation task before a restricted deadline remains unexplored under the interference channels. In this letter, we focus on the Nakagami-m fading channel and propose an analytical framework to characterize the reliability of computation offloading with the restrictions of application deadline and offloading data size in the presence of coupled stochastic interferences. A lower-bound offloading reliability capturing coupled randomness is theoretically derived. Based on the analytical framework, we further propose an admission control method for users to make computation offloading decisions. Simulation results verify our theoretical framework and show the superior performance of the proposed method over other benchmark schemes in terms of guaranteeing reliability.**

***Index Terms*—Mobile edge computing, computation offloading, Nakagami fading, wireless interference, admission control.**

I. Introduction

MOBILE edge computing (MEC) has been considered as an emerging paradigm for enabling a wide variety of existing and envisioned application scenarios. In any MEC-enabled systems, the decision-making of computation offloading is critical for their practical realization [1]. Many researchers are currently engaged in developing innovative computation offloading solutions such as the successive convex approximation (SCA) methods [2], the reinforcement learning or stochastic learning based methods [3]–[5]. Besides, game-theoretical approaches, such as the partially observable stochastic game [6], the Stackelberg game [7], the hierarchical game [8], and the stochastic game [9], have also been exploited to design a Nash-equilibrium solution for multi-user computation offloading in diverse resource-limited environments.

Meanwhile, reliability is an important requirement for data-massive and latency-aware end-to-end communications between end users and their targeted network edges. There are many factors needed to be handled for practically guaranteeing the reliability of computation offloading, among which the coupling, stochastic, and dynamic nature of physical-layer wireless interferences is the fundamental but most significant challenge. However, the coupled stochastic interferences from the physical layer has been largely neglected in most existing literature [2]–[9] and therein. Despite many state-of-the-art decision-making paradigms developed with well-known learning and optimization theories, few research efforts have been made to theoretically characterize the reliability of computation offloading and incorporate the reliability into decision-making in the presence of coupled stochastic interferences.

In this letter, we focus on the reliability modeling by capturing coupled stochastic interferences. Specifically, we exploit the commonly-adopted Nakagami-m distribution to model the small-scale fading of radio propagation due to the fact that it is shown to well capture the channel fading in various high-mobility wireless communication networks, such as vehicular networks [10], [11], unmanned aerial vehicles (UAV)-assisted networks [12], [13], multiple-input multiple-output (MIMO) and code division multiple access (CDMA) networks [14], [15]. Besides, the Nakagami-m distribution can also represent two specific cases such as the Rayleigh and Rician fading since it has high flexibility in channel modeling via tunning the parameter m. Based on the above channel model, we develop an analytical framework for the reliability of computation offloading. An admission control method based on a derived reliability bound is proposed to make effective computation offloading decisions while guaranteeing its success probability under both the deadline and demand restrictions. Simulations have also been conducted to show its effectiveness and superior reliability over benchmark schemes.

II. System Model

We focus on a general small-scale fading environment where the fading of radio propagation and the fluctuations of the signal envelope at receivers can be well characterized by the Nakagami distribution with parameter m. To be specific, let a random variable S_i be the received signal envelope

This research was supported in part by the National Postdoctoral Program for Innovative Talents under Grant No. BX2021027, the China Postdoctoral Science Foundation under Grant No. 2020M680299, the "Zhuoyue" Program of Beihang University under Grant No. 262716, the National Natural Science Foundation of China under Grant No. 61822101 and U20A20155, the Beijing Municipal Natural Science Foundation under Grant No. L191001, and the Newton Advanced Fellowship under Grant No. 62061130221. (Corresponding author: Jianshan Zhou.)

Guixian Qu, Jianshan Zhou, Haiyang Yu, and Yilong Ren are with Beijing Advanced Innovation Center for Big Data and Brain Computing, Beijing Key Laboratory for Cooperative Vehicle Infrastructure Systems & Safety Control, School of Transportation Science and Engineering, Beihang University, Beijing 100191, China (e-mail: guixianqu@foxmail.com, jianshanzhou@foxmail.com, hyyu@buaa.edu.cn, yilongren@buaa.edu.cn).

Zhengguo Sheng is with Department of Engineering and Design, the University of Sussex, Richmond 3A09, UK (e-mail: z.sheng@sussex.ac.uk).

from an end transmitter i of a computation offloading session, which follows a Nakagami distribution with two characteristic parameters (m_i, ω_i). The probability density function (PDF) of S_i is given as follows

$$f_{S_i}(s; m_i, \omega_i) = \frac{2m_i^{m_i}}{\Gamma(m_i)\,\omega_i^{m_i}} s^{2m_i-1} \exp\left(-\frac{m_i}{\omega_i} s^2\right), \quad (1)$$

where $m_i \in [0.5, 5]$ denotes the fading parameter, ω_i denotes the average power of the received signal envelope, and $\Gamma(m_i)$ is the Gamma function $\Gamma(m_i) = \int_0^\infty x^{m_i-1}\exp(-x)\mathrm{d}x$ [10]–[15]. Let P_i be the random received power from transmitter i and its PDF be $f_{P_i}(p)$. The relationship between the received power and the received signal envelope is $P_i = S_i^2$. At this point, we have the following lemma:

Lemma 1: The received power P_i follows a Gamma distribution and the PDF of P_i can be derived as $f_{P_i}(p) = \frac{1}{2}p^{-\frac{1}{2}} f_{S_i}(\sqrt{p}; m_i, \omega_i)$, i.e., $P_i \sim \mathrm{Gamma}(m_i, \omega_i)$.

Let a random variable I_j denote the interference power of j-th concurrent offloading session in close proximity to transmitter i and $j \in \mathcal{M}_i$, where $\mathcal{M}_i$ denotes the set of total physical-layer stochastic interferences to i's computation offloading. The sum of stochastic concurrent interferences received at i is then $Y_i = \sum_{j\in\mathcal{M}_i} I_j$. As in the Nakagami fading environment, each power interference I_j also follows a Gamma distribution with another parameters (m_j, ω_j) different from i's, i.e., $I_j \sim \mathrm{Gamma}(m_j, \omega_j)$. Let $M_i = |\mathcal{M}_i|$ be the cardinality of $\mathcal{M}_i$. For the sake of the generality, we consider that M_i stochastic interferences are independently non-identically distributed, i.e., $m_{j'}$ $(\omega_{j'})$ may not be identical to another one $m_{j''}$ $(\omega_{j''})$ for $j' \neq j''$ and $j', j'' \in \mathcal{M}_i$. Denoting the background noise power of i by N_i^2 in the Nakagami fading channel, we can formulate the signal to interference plus noise ratio (SINR) of the computation offloading link associated with i as follows

$$\phi(P_i, Y_i, N_i) = \frac{P_i}{N_i^2 + \sum_{j\in\mathcal{M}_i} I_j} = \frac{P_i}{N_i^2 + Y_i}, \quad (2)$$

which is indeed a compound random variable that incorporates the coupled stochastic dynamics of the concurrent interferences Y_i, the i's received power P_i, and the noise power N_i^2.

Lemma 2 ([16]): Given $I_j \sim \mathrm{Gamma}(m_j, \omega_j)$ for $j \in \mathcal{M}_i$ and let $f_{Y_i}(y)$ denote the PDF of Y_i, $f_{Y_i}(y)$ is expressed by

$$f_{Y_i}(y) = C \sum_{k=0}^{\infty} \frac{a_k y^{\alpha+k-1} \exp\left(-\frac{y}{b_1}\right)}{b_1^{(\alpha+k)}\Gamma(\alpha+k)}, \quad (3)$$

where the parameters are given as $\alpha = \sum_{j\in\mathcal{M}_i} m_j$, $b_j = \frac{\omega_j}{m_j}$, $b_1 = \min_{j\in\mathcal{M}_i}\{b_j\}$, $C = \prod_{j\in\mathcal{M}_i}\left(\frac{b_1}{b_j}\right)^{m_j}$ and

$$\begin{cases} a_0 = 1; \\ a_{k+1} = \dfrac{1}{k+1}\displaystyle\sum_{s=1}^{k+1}\left[\sum_{j\in\mathcal{M}_i} m_j\left(1-\frac{b_1}{b_j}\right)^s\right] a_{k+1-s} \\ k = 0, 1, \ldots \end{cases} \quad (4)$$

In addition, given an observation on the noise power N_i^2 as σ_i^2, i.e., $N_i^2 = \sigma_i^2$, and let $Z_i = \sigma_i^2 + Y_i$, the PDF of the linear combination, $f_{Z_i}(z)$, is $f_{Z_i}(z) = f_{Y_i}(z - \sigma_i^2)$.

Based on Lemmas 1 and 2, we further derive the following results. The proof of Theorem 1 is detailed in Appendix C available in the online supplementary material.

Theorem 1: Let $f_{\mathrm{SINR}}(\phi; \sigma_i)$ denote the PDF of the SINR $\phi(P_i, Y_i, N_i)$ under the condition that N_i^2 is observed to be $N_i^2 = \sigma_i^2$. $f_{\mathrm{SINR}}(\phi; \sigma_i)$ can be formulated as follows

$$f_{\mathrm{SINR}}(\phi; \sigma_i) = \int_{-\infty}^{+\infty} \frac{|z| f_{S_i}\left(\sqrt{z\phi}; m_i, \omega_i\right) f_{Y_i}\left(z - \sigma_i^2\right)}{2\sqrt{z\phi}} \mathrm{d}z. \quad (5)$$

For the practical system implementation, the time horizon is discretized into a series of slots each with the duration of $\Delta\tau$. Each time slot is indexed by t. We also consider to capture the stochastic dynamics of the received noise power N_i^2 into the offloading decision-making. For this goal, let $N_i^2(t)$ be the noise power in time slot t, and we quantize it into n different levels, i.e., $N_i^2(t) \in \{\sigma_{i,k}^2, k = 1, 2, \ldots, n\}$ where $\sigma_{i,k}^2$ is the noise power level in the k-th state, and model the stochastic transition between any two levels by a Markov chain with n states as shown in Figure 1. The transition probability of the noise power N_i^2 from $\sigma_{i,k'}^2$ to $\sigma_{i,k''}^2$ during time slot t is denoted by $p_{i,k'',k'} = \mathrm{Prob}\{N_i^2(t) = \sigma_{i,k''}^2 | N_i^2(t-1) = \sigma_{i,k'}^2\}$ for $k', k'' = 1, 2, \ldots, n$. At this point, we let $\mathbf{P}_i$ denote the transition probability matrix, i.e., $\mathbf{P}_i = [p_{i,k'',k'}] \in \mathbb{R}^{n\times n}$, and $\boldsymbol{\beta}_i = \mathrm{col}\{\beta_{i,k}, k = 1, 2, \ldots, n\}$ denote the steady state probability vector, where the element $\beta_{i,k}$ is the steady state probability that the received noise power N_i^2 is in the k-th state with the amplitude of $\sigma_{i,k}^2$. By using Markov chain theory, we can obtain the steady probability distribution $\boldsymbol{\beta}_i$ by solving

$$\boldsymbol{\beta}_i^{\mathrm{T}}\mathbf{P}_i = \boldsymbol{\beta}_i^{\mathrm{T}}, \ \boldsymbol{\beta}_i^{\mathrm{T}}\mathbf{1} = 1. \quad (6)$$

It is remarked that when the Markov chain has only one state, it boils down to a special case with a constant noise power.

III. Reliability of Computation Offloading

For simplicity of notation, we omit the time index t for the random process variables such as P_i, N_i, and I_j $(j \in \mathcal{M}_i)$ in the following derivations. Let D_i denote the total offloading data volume of i's application to the network edge and $T_i\Delta\tau$ denote its total tolerant latency, where T_i is the total number of the allowed time slots. It is expected that D_i should be fully offloaded to the edge by the deadline $T_i\Delta\tau$. Based on the SINR in (2), we can formulate the data rate of computation offloading associated with i using Shannon's theory as follows

$$\mathcal{R}_i(P_i, Y_i, N_i) = B\log_2\left(1 + \frac{P_i}{N_i^2 + \sum_{j\in\mathcal{M}_i} I_j}\right), \quad (7)$$

where B is the available bandwidth. In addition, the total data volume that can be offloaded by i to the network edge within a constrained time window $[0, T_i\Delta\tau]$ is derived as

$$\Theta(P_i, Y_i, N_i) = \sum_{t=1}^{T_i} \mathcal{R}_i(P_i, Y_i, N_i)\Delta\tau. \quad (8)$$

Based on (8), we can characterize the reliability of computation offloading as the success probability of mobile user i offloading D_i-bit data to the network edge by a specified deadline $T_i\Delta\tau$, which can be formulated as $\mathrm{Prob}\{\Theta(P_i, Y_i, N_i) >$

$D_i\}$ from a probabilistic perspective. For simplicity, let $\varphi(T_i, D_i) = \text{Prob}\{\Theta(P_i, Y_i, N_i) > D_i\}$. Note that (8) involves the integration of multiple coupled random processes. In fact, it is intractable to obtain a deterministic value of the offloaded data volume under the deadline constraint, $\Theta(P_i, Y_i, N_i)$. Instead, we first derive the mathematical expectation and an upper-bound variance of $\Theta(P_i, Y_i, N_i)$ based on the probability models of the SINR $\phi(P_i, Y_i, N_i)$ and the noise power N_i^2 in Section II. Based on this, we further derive a lower-bound success probability $\varphi(T_i, D_i)$, i.e., the lower bound of the offloading reliability. Given $N_i^2 = \sigma_i^2$, we let $\mathcal{R}_i(\phi; \sigma_i)$ denote an observation on $\mathcal{R}_i(P_i, Y_i, N_i)$, where $\mathcal{R}_i(\phi; \sigma_i) = B \log_2(1+\phi)$. Thus, we get the following result:

Theorem 2: The mathematical expectation of $\Theta(P_i, Y_i, N_i)$ is derive as

$$\mathbb{E}\left[\Theta(P_i, Y_i, N_i)\right] = \sum_{t=1}^{T_i} \mathbb{E}\left[\mathcal{R}_i(P_i, Y_i, N_i)\right] \Delta\tau, \tag{9}$$

where $\mathbb{E}\left[\mathcal{R}_i(P_i, Y_i, N_i)\right]$ is given by

$$\begin{aligned} &\mathbb{E}\left[\mathcal{R}_i(P_i, Y_i, N_i)\right] \\ &= \int_0^\infty \sum_{k=1}^{n} \mathcal{R}_i(\phi; \sigma_{i,k}) \beta_{i,k}(t) f_{\text{SINR}}(\phi; \sigma_{i,k}) \mathrm{d}\phi, \end{aligned} \tag{10}$$

and the variance of $\Theta(P_i, Y_i, N_i)$ is upper bounded by

$$\begin{aligned} \text{Var}\left[\Theta(P_i, Y_i, N_i)\right] \le T_i \left(\Delta\tau\right)^2 \sum_{t=1}^{T_i} \mathbb{E}\left[\mathcal{R}_i^2(P_i, Y_i, N_i)\right] \\ - \left(\mathbb{E}\left[\Theta(P_i, Y_i, N_i)\right]\right)^2, \end{aligned} \tag{11}$$

where $\mathbb{E}\left[\mathcal{R}_i^2(P_i, Y_i, N_i)\right]$ is given by

$$\begin{aligned} &\mathbb{E}\left[\mathcal{R}_i^2(P_i, Y_i, N_i)\right] \\ &= \int_0^\infty \sum_{k=1}^{n} \mathcal{R}_i^2(\phi; \sigma_{i,k}) \beta_{i,k}(t) f_{\text{SINR}}(\phi; \sigma_{i,k}) \mathrm{d}\phi. \end{aligned} \tag{12}$$

For simplicity, we let $\text{Var}^{\text{upper}}\left[\Theta(P_i, Y_i, N_i)\right]$ represent the upper bound of the variance of $\Theta(P_i, Y_i, N_i)$ as given in (11), i.e., $\text{Var}\left[\Theta(P_i, Y_i, N_i)\right] \le \text{Var}^{\text{upper}}\left[\Theta(P_i, Y_i, N_i)\right]$. Moreover, we derive a lower bound on $\varphi\left(T_i, D_i\right)$ as follows.

Theorem 3: Let $\varphi^{\text{lower}}\left(T_i, D_i\right)$ denote a lower bound of $\varphi\left(T_i, D_i\right)$, i.e., $\varphi^{\text{lower}}\left(T_i, D_i\right) \le \varphi\left(T_i, D_i\right)$. $\varphi^{\text{lower}}\left(T_i, D_i\right)$ can be given by

$$\varphi^{\text{lower}}\left(T_i, D_i\right) = \frac{\left(\mathbb{E}\left[\Theta(P_i, Y_i, N_i)\right] - D_i\right)^2}{\text{Var}^{\text{upper}}\left[\Theta(P_i, Y_i, N_i)\right] + \left(\mathbb{E}\left[\Theta(P_i, Y_i, N_i)\right] - D_i\right)^2} \tag{13}$$

with $\mathbb{E}\left[\Theta(P_i, Y_i, N_i)\right] > D_i$.

It is remarked that the proofs of both Theorems 2 and 3 are elaborated on in Appendices D and E, respectively, which are provided in the online supplementary material.

IV. Admission Control Design

Now, by using the results of Theorems 1 to 3 above, we can design a threshold-based admission control policy for making computation offloading decisions. To be specific, let a predefined threshold be η_i, where $0 \ll \eta_i < 1$, for computation offloading decision-making. The mobile user i is encouraged to offload its computation task with D_i-bit data within T_i time slots if both the following designed conditions are satisfied:

$$\mathbb{E}\left[\Theta(P_i, Y_i, N_i)\right] > D_i \text{ and } \varphi^{\text{lower}}\left(T_i, D_i\right) \ge \eta_i; \tag{14}$$

Otherwise, the mobile user i should buffer the computation task and process it locally since its computation offloading is more likely to fail due to the intermittent communication.

Fig. 1 provides an implementation framework illustrating how our admission control can be practically deployed in an actual situation. Fig. 2 gives a typical application for vehicular object detection assisted with MEC for the sake of demonstration. Our admission control enables the user to adaptively decide whether to offload or not according to its

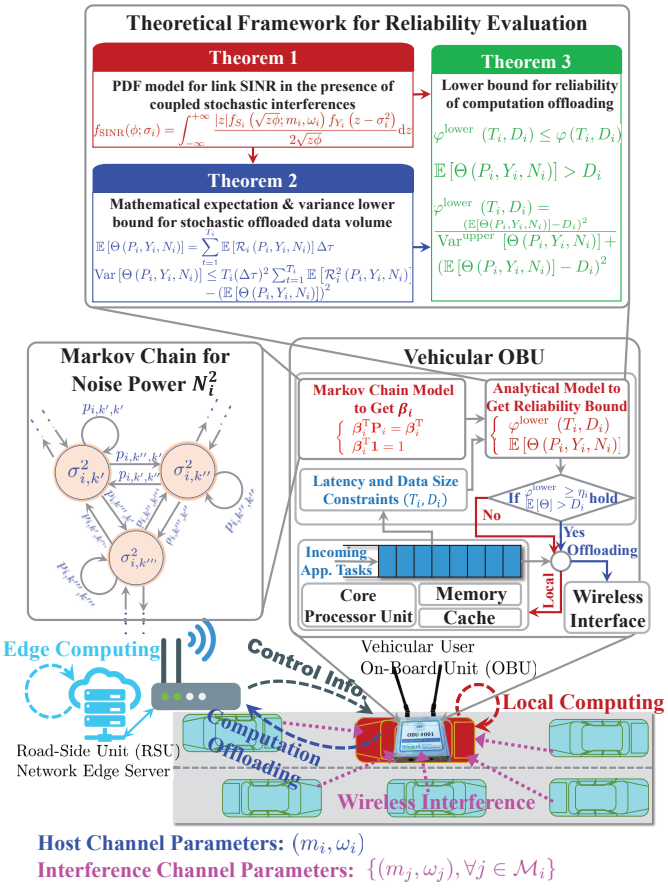

Fig. 1. The implementation framework using our admission control for computation offloading in an exemplary MEC-enabled vehicular network.

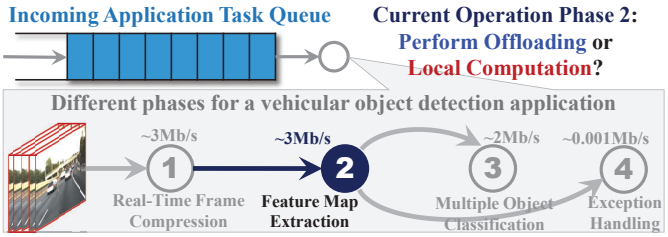

Fig. 2. An exemplary application of computation offloading for vehicular object detection where the user can decide to offload parts of the operation program (i.e., an operation phase) to the edge nearby for remote computation.

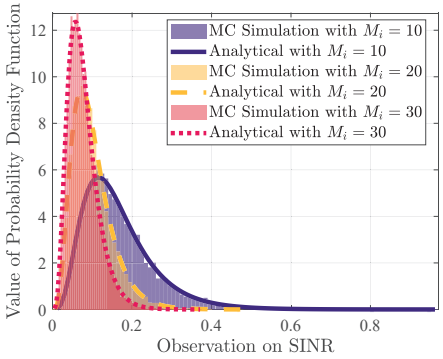

Fig. 3. The PDF of the SINR under coupled stochastic interferences.

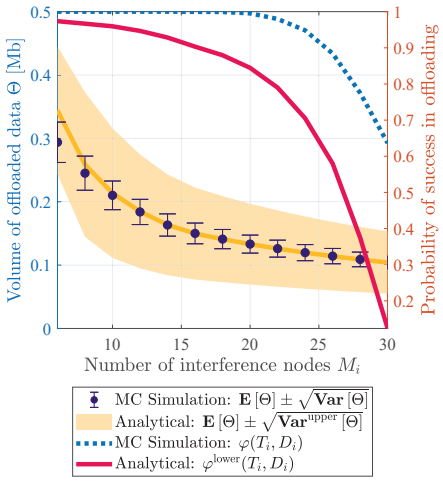

Fig. 4. The capacity of computation offloading and the success probability of offloading D_i-bit data within $[0, T_i\Delta\tau]$.

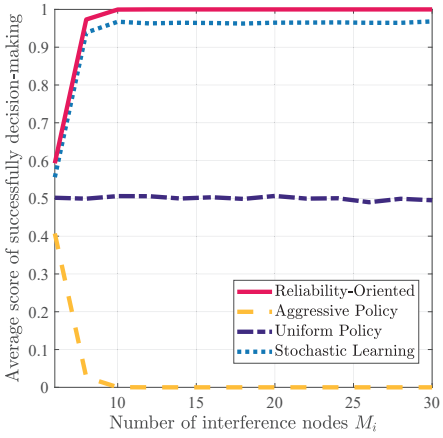

Fig. 5. The performance comparison in terms of the score of successfully decision-making under different numbers of interference nodes.

application demand, deadline constraint, and evaluated lower-bound reliability. When the threshold condition (14) is met, indicating that the user is more likely to successfully complete the data-massive and latency-constrained computation offloading, i.e., guaranteeing the transmission content integrity with a high reliability, he is encouraged to offload its computation. Otherwise, he should adopt the local computation mode.

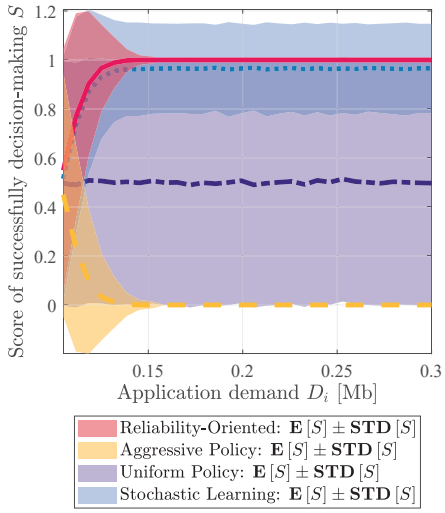

Fig. 6. The performance comparison in terms of the score of successfully decision-making under different application demands.

V. Simulation Experiment

In this section, we provide simulation results to verify the proposed models and admission control method. Here, the parameter settings are referred to in a vehicular communication scenario [10], [11]. The bandwidth is set as $B = 10$ Mb/Hz/s. The parameters of the Nakagami channel for the host transmitter i's computation offloading is set as $m_i = 5$ and $\omega_i = 1$. The inter-distance between any two successive interference nodes is randomly generated by following an exponential distribution with the average space headway of 20 m, and the channel parameters of each interference node $j \in \mathcal{M}_i$, m_j and ω_j, are set as a function of its relative distance from itself to i's receiver. The relative interference distance-based channel parameters are detailed in our online supplementary material, which are based on the field measurements in [10]. The noise power level is divided into 3 states, i.e., $N_i^2(t) \in \{-95, 0, 30\}$ dBm and the transition probability matrix $\mathbf{P}_i$ is given as

$$\mathbf{P}_i = \begin{bmatrix} 0.7 & 0.2 & 0.1 \\ 0.2 & 0.6 & 0.2 \\ 0.3 & 0.2 & 0.5 \end{bmatrix}. \tag{15}$$

The duration per time slot is $\Delta\tau = 5$ ms and the allowed latency for an application is restricted to 100 ms, i.e., $T_i = 20$. The application demand is $D_i = 0.1 \times 10^6$ bits. η_i is generated by following a uniform distribution on the interval $[0, 1]$, i.e., $\eta_i \sim \mathcal{U}(0, 1)$. We have conducted extensive Monte Carlo (MC) simulation experiments. All the MC simulations in this letter have been performed with 10^4 replications per condition.

In Fig. 3 and Fig. 4, we validate our theoretical results as given in Theorems 1, 2 and 3 for modeling the analytical SINR PDF, $f_{\text{SINR}}(\phi; \sigma_i)$, the mean and upper-bound variance of the offloading capacity, $\mathbb{E}[\Theta]$ and $\text{Var}^{\text{upper}}[\Theta]$, and the lower bound of the reliability of computation offloading, $\varphi^{\text{lower}}(T_i, D_i)$, under different numbers of interference nodes, M_i. It is seen from Fig. 3 that our analytical model can well characterize the actual SINR distribution obtained by the MC simulations. The mean square error between the MC simulation and the

analytical results is about 0.09% under $M_i = 10$, 0.11% under $M_i = 20$, and 0.05% under $M_i = 30$, respectively. From Fig. 4, the volume of data that can be offloaded under the Nakagami channel with multiple coupled stochastic interferences is reduced with the increasing interference nodes. The probability of success in computation offloading also degrades when the coupled interferences are enhanced. Besides, Fig. 4 shows that the analytical model (9) can well approximate the mathematical expectation of the offloaded data volume Θ, $\mathbb{E}[\Theta]$, and (9) can provide an upper bound for its variance, $\mathrm{Var}^{\mathrm{upper}}[\Theta]$. The offloading capacity, Θ, is bounded within the derived interval characterized by $\mathbb{E}[\Theta] \pm \sqrt{\mathrm{Var}^{\mathrm{upper}}[\Theta]}$ with the confidence of 100%. In Fig. 4, the analytical model (13), $\varphi^{\mathrm{lower}}(T_i, D_i)$, is also shown to always provide a lower bound on the reliability of computation offloading under different coupled stochastic interferences.

Moreover, we compare our admission control method for offloading decision-making with some other methods including the aggressive policy- and the uniform policy-based methods, and the stochastic learning-based method[1]. We introduce a score metric S to comprehensively indicate the performance of the node's decision-making in a stochastic environment. S is set to 1 if i can make a correct decision, i.e., it chooses to offload its application when $\Theta \geq D_i$ or to buffer the application when $\Theta \leq D_i$. Otherwise, S is set to 0 if i makes a wrong decision, i.e., it chooses the remote computation when $\Theta < D_i$ or the local computation when $\Theta > D_i$.

In Fig. 5, the application demand is set to $D_i = 0.3 \times 10^6$ bits and M_i is ranged from 6 to 30. From Fig. 5, the average score of successfully decision-making under our proposed admission control and the stochastic learning method can increase even when the coupled interference nodes are increased. On the contrary, the performance of the aggressive policy degrades due to the increasing interference effect, while that of the uniform policy is only about 0.5 since it exploits a fixed 50% offloading strategy. From Fig. 5, the score of making correct decisions using our proposed method is about 3.86% higher than that of the stochastic learning method on average. In Fig. 6, we fix M_i at $M_i = 30$ and then compare the different methods by increasing D_i from about 0.1 Mb to 0.3 Mb. Their scores are demonstrated with the standard deviation intervals. It is also found that our proposed method can outperform the others. Specifically, the admission control method can boost the mean correct decision-making score of about 3.79% over the stochastic learning method. In particular, the standard deviation of the admission control-based decision-making performance gradually converges to zero, while those of the stochastic learning method and the uniform policy are maintained around 0.21 and 0.49, respectively. This indicates that our method can narrow the decision-making uncertainty even when increasing the application demand, i.e., reducing the risk in making wrong decisions on computation offloading.

[1]The aggressive policy motives the node to always offload its application. When using the uniform policy, the node decides to offload with 50% probability. With the stochastic learning method, the node makes an offloading decision based on a dynamic probability $p_i(t)$, and the offloading probability can be dynamically adapted according to the linear reward-inaction mechanism. The details on the implementation of the stochastic learning method can be found in Appendix G available in the online supplementary material.

VI. CONCLUSION

In this letter, we have proposed a theoretical model to derive a lower-bound reliability of computation offloading by jointly considering the stochastic interferences under the Nakagami channel. We have designed a reliability-guaranteed admission control method. Simulations verify its superior performance over several other schemes. In future work, we aim to develop a secure optimization framework for blockchain-enabled MEC by extending our reliability-guaranteed admission control with artificial intelligence (AI)-driven resource scheduling.

REFERENCES

[1] Y. Mao, C. You, J. Zhang, K. Huang, and K. B. Letaief, "A survey on mobile edge computing: The communication perspective," *IEEE Communications Surveys Tutorials*, vol. 19, no. 4, pp. 2322–2358, Fourthquarter 2017.

[2] M. Li, N. Cheng, J. Gao, Y. Wang, L. Zhao, and X. Shen, "Energy-efficient uav-assisted mobile edge computing: Resource allocation and trajectory optimization," *IEEE Transactions on Vehicular Technology*, vol. 69, no. 3, pp. 3424–3438, March 2020.

[3] N. Cheng, F. Lyu, W. Quan, C. Zhou, H. He, W. Shi, and X. Shen, "Space/aerial-assisted computing offloading for iot applications: A learning-based approach," *IEEE Journal on Selected Areas in Communications*, vol. 37, no. 5, pp. 1117–1129, May 2019.

[4] X. Qiu, L. Liu, W. Chen, Z. Hong, and Z. Zheng, "Online deep reinforcement learning for computation offloading in blockchain-empowered mobile edge computing," *IEEE Transactions on Vehicular Technology*, vol. 68, no. 8, pp. 8050–8062, Aug 2019.

[5] R. Zhang, P. Cheng, Z. Chen, S. Liu, Y. Li, and B. Vucetic, "Online learning enabled task offloading for vehicular edge computing," *IEEE Wireless Communications Letters*, vol. 9, no. 7, pp. 928–932, July 2020.

[6] Q. Tang, R. Xie, T. Huang, W. Feng, and Y. Liu, "Dynamic computation offloading with imperfect state information in energy harvesting small cell networks: A partially observable stochastic game," *IEEE Wireless Communications Letters*, vol. 9, no. 8, pp. 1300–1304, Aug 2020.

[7] M. Liu and Y. Liu, "Price-based distributed offloading for mobile-edge computing with computation capacity constraints," *IEEE Wireless Communications Letters*, vol. 7, no. 3, pp. 420–423, June 2018.

[8] A. Asheralieva and D. Niyato, "Hierarchical game-theoretic and reinforcement learning framework for computational offloading in uav-enabled mobile edge computing networks with multiple service providers," *IEEE Internet of Things Journal*, vol. 6, no. 5, pp. 8753–8769, Oct 2019.

[9] J. Zheng, Y. Cai, Y. Wu, and X. Shen, "Dynamic computation offloading for mobile cloud computing: A stochastic game-theoretic approach," *IEEE Transactions on Mobile Computing*, vol. 18, no. 4, pp. 771–786, April 2019.

[10] L. Cheng, B. E. Henty, D. D. Stancil, F. Bai, and P. Mudalige, "Mobile vehicle-to-vehicle narrow-band channel measurement and characterization of the 5.9 ghz dedicated short range communication (dsrc) frequency band," *IEEE Journal on Selected Areas in Communications*, vol. 25, no. 8, pp. 1501–1516, Oct 2007.

[11] R. He, A. F. Molisch, F. Tufvesson, Z. Zhong, B. Ai, and T. Zhang, "Vehicle-to-vehicle propagation models with large vehicle obstructions," *IEEE Transactions on Intelligent Transportation Systems*, vol. 15, no. 5, pp. 2237–2248, Oct 2014.

[12] A. A. Khuwaja, Y. Chen, and G. Zheng, "Effect of user mobility and channel fading on the outage performance of uav communications," *IEEE Wireless Communications Letters*, vol. 9, no. 3, pp. 367–370, March 2020.

[13] P. K. Sharma and D. I. Kim, "Coverage probability of 3-d mobile uav networks," *IEEE Wireless Communications Letters*, vol. 8, no. 1, pp. 97–100, Feb 2019.

[14] G. Fraidenraich, O. Leveque, and J. M. Cioffi, "On the mimo channel capacity for the nakagami-m channel," *IEEE Transactions on Information Theory*, vol. 54, no. 8, pp. 3752–3757, Aug 2008.

[15] P. Sedtheetorn, K. A. Hamdi, and L. Wuttisittikuljit, "Theoretical analysis on bit error rate of vsg cdma in nakagami fading," *IEEE Transactions on Information Theory*, vol. 57, no. 6, pp. 3405–3410, June 2011.

[16] P. G. Moschopoulos, "The distribution of the sum of independent gamma random variables," *Annals of the Institute of Statistical Mathematics*, vol. 1, no. 6, pp. 541–544, 1985.

Supplementary Material for Reliability-Guaranteed Admission Control for Mobile Computation Offloading under Nakagami Fading Channel

Guixian Qu, Jianshan Zhou, Zhengguo Sheng, *Senior Member, IEEE*, Haiyang Yu, and Yilong Ren

Remark: The online supplementary material elaborates on the proofs of Lemmas 1 to 2, and Theorems 1 to 3. In addition, the implementation of the stochastic learning method adopted in the simulation experiments is also detailed.

Appendix A
Proof of Lemma 1

Based on the PDF of S_i as in (1), $f_{S_i}(x; m_i, \omega_i)$, we can derive the cumulative distribution function (CDF) of i's received power $P_i = S_i^2$ as follows

$$\text{Prob}\{P_i \le p\} = \text{Prob}\{S_i \le \sqrt{p}\} = \frac{\gamma\left(m_i, \frac{m_i}{\omega_i}p\right)}{\Gamma(m_i)}, \quad \text{(S.1)}$$

where $\gamma(m_i, x) := \int_0^x s^{m_i-1}\exp(-s)ds$. Using (S.1), we obtain the PDF of P_i by differentiating its PDF as follows

$$f_{P_i}(p) = \frac{d\text{Prob}\left\{S_i \le \sqrt{p}\right\}}{dp} = \frac{1}{2}\frac{f_{S_i}\left(\sqrt{p}; m_i, \omega_i\right)}{\sqrt{p}}, \quad \text{(S.2)}$$

which indicates that P_i follows a Gamma distribution with the parameters m_i and ω_i, i.e., $P_i \sim \text{Gamma}(m_i, \omega_i)$. At this point, Lemma 1 is proven.

Appendix B
Proof of Lemma 2

In fact, Lemma 2 states an exact PDF of the sum of finite and mutually independent Gamma-distributed random variables, which is originally presented by P. G. Moschopoulos [1]. The key idea to derive the PDF is realized by inverting the corresponding moment generating function (MGF). Specifically, the MGF of $Y_i = \sum_{j\in\mathcal{M}_i} I_j$ is the product of those of I_j $(j \in \mathcal{M}_i)$, i.e.,

$$M(t) = \prod_{j\in\mathcal{M}_i}\left(1 - \frac{\omega_j}{m_j}t\right)^{-m_j}. \quad \text{(S.3)}$$

As shown in [1], (S.3) can be further re-arranged as the following form by using the notations defined in Lemma 2

$$M(t) = C\left(1 - b_1 t\right)^{-\alpha}\exp\left(\sum_{k=1}^{\infty}\gamma_k\left(1 - b_1 t\right)^{-k}\right), \quad \text{(S.4)}$$

where γ_k is defined as

$$\gamma_k = \sum_{j\in\mathcal{M}_i}\frac{m_j\left(1 - \frac{b_1}{b_j}\right)^k}{k}, \text{ for } k = 1, 2, \ldots. \quad \text{(S.5)}$$

By letting

$$\exp\left(\sum_{k=1}^{\infty}\gamma_k\left(1 - b_1 t\right)^{-k}\right) = \sum_{k=0}^{\infty}a_k\left(1 - b_1 t\right)^{-k} \quad \text{(S.6)}$$

and inverting the MGF of Y_i, (S.4), term-by-term, we can finally derive the PDF of Y_i as stated in Lemma 2. It should be remarked that interested readers can refer to [1] for more details on the relevant mathematical derivation.

Appendix C
Proof of Theorem 1

Let $F_{\text{SINR}}(\phi; \sigma_i)$ be the cumulative density function (CDF) of $\phi(P_i, Y_i, N_i)$. According to the definition of the CDF, we have

$$\begin{aligned} F_{\text{SINR}}(\phi;\sigma_i) &= \text{Prob}\{\phi(P_i, Y_i, \sigma_i) \le \phi\} \\ &= \text{Prob}\{P_i \ge Z_i\phi, Z_i < 0\} \\ &\quad + \text{Prob}\{P_i \le Z_i\phi, Z_i > 0\} \\ &= \int_{-\infty}^{0}\left(\int_{z\phi}^{+\infty} f_{P_i}(p)\text{d}p\right) f_{Z_i}(z)\text{d}z \\ &\quad + \int_{0}^{\infty}\left(\int_{-\infty}^{z\phi} f_{P_i}(p)\text{d}p\right) f_{Z_i}(z)\text{d}z. \end{aligned} \quad \text{(S.7)}$$

By differentiating (S.7), we can further get

$$\begin{aligned} f_{\text{SINR}}(\phi;\sigma_i) &= \frac{\text{d}F_{\text{SINR}}(\phi;\sigma_i)}{\text{d}\phi} \\ &= \int_{-\infty}^{0}\left(-z f_{P_i}(z\phi)\right) f_{Z_i}(z)\text{d}z \\ &\quad + \int_{0}^{+\infty}\left(z f_{P_i}(z\phi)\right) f_{Z_i}(z)\text{d}z \\ &= \int_{-\infty}^{+\infty}|z| f_{P_i}(z\phi) f_{Z_i}(z)\text{d}z. \end{aligned} \quad \text{(S.8)}$$

Substituting $f_{P_i}(p) = \frac{1}{2}p^{-\frac{1}{2}}f_{S_i}(\sqrt{p}; m_i, \omega_i)$ and the results of Lemmas 1 and 2 into (S.8) can prove Theorem 1.

Appendix D
Proof of Theorem 2

The results of (9), (10) and (12) simply follow the definition and basic property of the mathematical expectation. In the

following, we mainly prove (11). Recall the definition of the variance, we have

$$\begin{aligned}\mathrm{Var}\left[\Theta(P_i,Y_i,N_i)\right] =& \mathbb{E}\left[\Theta^2(P_i,Y_i,N_i)\right] \\ &- \left(\mathbb{E}\left[\Theta(P_i,Y_i,N_i)\right]\right)^2,\end{aligned} \tag{S.9}$$

where $\mathbb{E}\left[\Theta^2(P_i,Y_i,N_i)\right]$ can be further expressed as

$$\mathbb{E}\left[\Theta^2(P_i,Y_i,N_i)\right] = \mathbb{E}\left[\left(\sum_{t=1}^{T_i}\mathcal{R}_i(P_i,Y_i,N_i)\Delta\tau\right)^2\right]. \tag{S.10}$$

Using the Cauchy-Schwarz inequality, we can get

$$\begin{aligned}\left(\sum_{t=1}^{T_i}\mathcal{R}_i(P_i,Y_i,N_i)\Delta\tau\right)^2 &\le \left[\sum_{t=1}^{T_i}(\Delta\tau)^2\right]\left[\sum_{t=1}^{T_i}\mathcal{R}_i^2(P_i,Y_i,N_i)\right] \\ &= T_i\left(\Delta\tau\right)^2\sum_{t=1}^{T_i}\mathcal{R}_i^2(P_i,Y_i,N_i).\end{aligned} \tag{S.11}$$

Substituting (S.11) into (S.10) can immediately derive (11) and thus proves Theorem 2.

Appendix E
Proof of Theorem 3

Let $B = \mathbb{E}\left[\Theta(P_i,Y_i,N_i)\right] - \Theta(P_i,Y_i,N_i)$ and $b = \mathbb{E}\left[\Theta(P_i,Y_i,N_i)\right] - D_i$. It is noted that

$$\begin{aligned}\mathbb{E}[B] &= \mathbb{E}\left[\mathbb{E}\left[\Theta(P_i,Y_i,N_i)\right] - \Theta(P_i,Y_i,N_i)\right] \\ &= \mathbb{E}\left[\Theta(P_i,Y_i,N_i)\right] - \mathbb{E}\left[\Theta(P_i,Y_i,N_i)\right] = 0\end{aligned} \tag{S.12}$$

and

$$\begin{aligned}\varphi\left(T_i,D_i\right) &= \mathrm{Prob}\left\{\begin{matrix}\mathbb{E}\left[\Theta(P_i,Y_i,N_i)\right] - \Theta(P_i,Y_i,N_i) \\ < \mathbb{E}\left[\Theta(P_i,Y_i,N_i)\right] - D_i\end{matrix}\right\} \\ &= \mathrm{Prob}\left\{B < b\right\}.\end{aligned} \tag{S.13}$$

Besides, according to (S.12), we can see

$$b^2 = \left(b - \mathbb{E}[B]\right)^2 = \left(\mathbb{E}[b-B]\right)^2 \le \left(\mathbb{E}[(b-B)1_{b-B>0}]\right)^2 \tag{S.14}$$

where $1_{b-B>0}$ is an indicator satisfying $1_{b-B>0} = 1$ if and only if $b - B > 0$; otherwise, $1_{b-B>0} = 0$ for $b - B \le 0$. Applying the Cauchy-Schwarz inequality to (S.14) can further yield

$$\left(\mathbb{E}[(b-B)1_{b-B>0}]\right)^2 \le \mathbb{E}\left[(b-B)^2\right]\mathbb{E}\left[1_{b-B>0}^2\right]. \tag{S.15}$$

Notice that $\mathbb{E}\left[(b-B)^2\right] = \mathbb{E}\left[b^2 - 2bB + B^2\right] = b^2 + \mathbb{E}[B^2] = b^2 + \mathbb{E}[(\mathbb{E}\left[\Theta(P_i,Y_i,N_i)\right] - \Theta(P_i,Y_i,N_i))^2] = b^2 + \mathrm{Var}[\Theta(P_i,Y_i,N_i)]$ and $\mathbb{E}\left[1_{b-B>0}^2\right] = \mathrm{Prob}\{b > B\}$. Substituting the results into (S.15), we have

$$\mathrm{Prob}\{b > B\} \ge \frac{b^2}{b^2 + \mathrm{Var}\left[\Theta(P_i,Y_i,N_i)\right]}. \tag{S.16}$$

Combining (11), (S.13) and (S.16) immediately derives (13). At this point, Theorem 3 is proven.

TABLE I
Parameter m based on relative distance d (in meter) [2]

d	≤ 5.5	≤ 13.9	≤ 35.5	≤ 90.5	≤ 230.7	≤ 588.0
m	4.07	2.44	3.08	1.52	0.74	0.84

Appendix F
Parameter Settings on Nakagami Fading Channel

The physical-layer parameters, (m_i,ω_i), (m_j,ω_j), $j \in \mathcal{M}_i$, play a key role in the Nakagami fading channel. For properly conducting channel simulations, we consider a specific vehicular communication scenario as in [2], [3], in which the computation offloading is operated via vehicular communication links. To be specific, we refer to the field measurements as reported in [2] to configure the Nakagami fading channel in our simulation experiments. According to [2], the average received power in the fading envelope can be normalized to 1, while the fading parameter can range within $[0.5, 5]$, which relies on the relative distance between a transmitter and a receiver. The adopted fading parameters over different relative distances are detailed in TABLE I.

Besides, as presented in some other studies like [4], [5] based on field measurements, an exponential distribution can have a promising fit for describing the random distribution of inter-vehicle spacing in a common traffic environment. Hence, in our simulations, an exponential distribution with the average space headway of $20\,\mathrm{m}$ is specified to randomly generate the relative distances between the nodes, i.e., $d \sim \exp(\frac{1}{20})$.

Appendix G
Implementation of Stochastic Learning Method for Performance Comparison

In the simulation experiments, the user i can dynamically adapt its offloading probability $p_i(t)$ when he adopts the stochastic learning method. Specifically, $p_i(t)$ is updated according to the following linear reward-inaction mechanism:

$$p_i(t+\Delta\tau) = p_i(t) + \lambda_i S(t)\left[\mathbf{1}_{\text{offloading}}(t) - p_i(t)\right] \tag{S.17}$$

where λ_i is a learning rate and set to 10^{-3} in the experiments, $S(t)$ is the score metric gained at t, and $\mathbf{1}_{\text{offloading}}(t)$ is a $0-1$ indicator that is equal to 1 if and only if i chooses to offload its application at t, otherwise 0. It is remarked that the stochastic learning method follows an adaptive reinforcement mechanism and is known as an advanced method for distributed multi-agent decision-making in a dynamic and stochastic environment. Thus, it is used in this letter for the state-of-the-art performance comparison.

References

[1] P. G. Moschopoulos, "The distribution of the sum of independent gamma random variables," *Annals of the Institute of Statistical Mathematics*, vol. 1, no. 6, pp. 541–544, 1985.

[2] L. Cheng, B. E. Henty, D. D. Stancil, F. Bai, and P. Mudalige, "Mobile vehicle-to-vehicle narrow-band channel measurement and characterization of the 5.9 ghz dedicated short range communication (dsrc) frequency band," *IEEE Journal on Selected Areas in Communications*, vol. 25, no. 8, pp. 1501–1516, Oct 2007.

[3] R. He, A. F. Molisch, F. Tufvesson, Z. Zhong, B. Ai, and T. Zhang, "Vehicle-to-vehicle propagation models with large vehicle obstructions," *IEEE Transactions on Intelligent Transportation Systems*, vol. 15, no. 5, pp. 2237–2248, Oct 2014.

[4] H. Zhu, L. Fu, G. Xue, Y. Zhu, M. Li, and L. M. Ni, "Recognizing exponential inter-contact time in vanets," in *2010 Proceedings IEEE INFOCOM*, March 2010, pp. 1–5.

[5] N. Wisitpongphan, F. Bai, P. Mudalige, V. Sadekar, and O. Tonguz, "Routing in sparse vehicular ad hoc wireless networks," *IEEE Journal on Selected Areas in Communications*, vol. 25, no. 8, pp. 1538–1556, Oct 2007.